Autoresonant excitation and control of molecular degrees of freedom in three dimensions

Gilad Marcus, Lazar Friedland, and Arie Zigler
Racah Institute of Physics, Hebrew University of Jerusalem, Jerusalem 91904, Israel
(Received 5 April 2005; published 12 September 2005)

A classical, three-dimensional analysis of excitation and control of vibrational-rotational degrees of freedom of a polar diatomic molecule by chirped laser field is presented. The control strategy is based on autoresonance (adiabatic nonlinear synchronization) phenomenon, in which the molecule automatically adjusts its state for staying in a persistent resonance with the laser field despite variation of the laser frequency. Thresholds on driving field amplitudes for entering the autoresonant excitation regime by passage through different resonances are calculated. In autoresonance, the molecule can be excited to large energies and approach the dissociation limit by substantially weaker laser fields than with constant-frequency drives.

DOI: 10.1103/PhysRevA.72.033404 PACS number(s): 42.50.Hz, 33.80.Gj, 33.80.Wz

I. INTRODUCTION

Molecular dissociation without ionization or excitation of higher molecular vibrational levels is of great importance for the initiation of certain chemical reactions. For example, vibrational excitation along the reaction coordinate can yield increased reaction efficiency [1]. Direct excitation of high vibrational levels in a molecule by a monochromatic radiation is inefficient, due to the small value of the transition dipole moment between the initial and final states [2]. A strategy of climbing along the vibrational energy level ladder by a cascade of transitions was suggested [3] for overcoming this problem. In this scheme one first excites the molecule from the ground level to $\nu=1$ level, then from $\nu=1$ to $\nu=2$, and so on. The vibrational energy levels are not equally spaced due to unharmonicity, and, therefore, one must vary the laser frequency in this process of successive excitations. Also, it has been shown that the variation of the laser frequency for efficient multistep excitation can be continuous (chirped frequency laser light). Such a strategy to excite molecular vibrations was referred to as ladder climbing (LC). Other researchers employed classical analysis of atomic and molecular excitations by chirped laser radiation using the autoresonance (AR) phenomenon [4,5] to get more insight into the excitation dynamics, while the relation between the quantum-mechanical LC and classical AR was discussed recently in Ref. [6]. Most of the theoretical work in this field, either classical or quantum mechanical, employed a one-dimensional (1D) model, which neglected the coupling between vibrational and rotational degrees of freedom. Some authors argued (based primarily on numerical simulations) that in a real 3D case, where the rotational degree of freedom is playing an important role, the excitation efficiency drops dramatically due to vibrational-rotational (VR) coupling [7,8].

The present work uses ideas developed in studying 3D autoresonant control of Rydberg atoms [9] and presents a classical 3D theory of autoresonant excitation and control of molecular VR degrees of freedom by chirped laser radiation. The goal is to arrive at more solid conclusions about the role of rotations on the vibrational excitation efficiency and develop a strategy of controlling both vibrational and rotational degrees of freedom by chirped frequency laser fields.

Our presentation will be as follows. We shall formulate our 3D laser-driven dynamical problem in terms of molecular action-angle variables in Sec. II. This will yield the most convenient theoretical setting for studying adiabatic autoresonant interactions. Section III will describe the general theory of 3D autoresonant control of polar diatomic molecules and apply this theory to specific examples. In particular, we shall focus on rotational and rotational-vibrational controls of a diatomic molecule described by the Morse potential. The important issue of passage through resonances and autoresonant synchronization in driven molecular systems will be discussed in Sec. IV. The synchronization thresholds by passage through resonance in different excitation scenarios will be calculated in the same section and our theoretical predictions will be tested in numerical simulations. Finally, Sec. V will summarize our results.

II. ACTION-ANGLE FORMALISM

Our starting point is the classical, 3D Hamiltonian describing a diatomic, polar molecule (in spherical coordinates; see the geometry in Fig. 1) in the laser field

$$H=\frac{1}{2\mu}\left(p_r^2+\frac{p_\theta^2}{r^2}+\frac{p_\varphi^2}{r^2\sin^2\theta}\right)+U_0(r)+U_1, \tag{1}$$

where μ is the reduced mass, r is the distance between the two atoms, $p_{r,\theta,\varphi}$ are different momentum components, $U_0(r)$ represents the potential interaction energy (we shall assume Morse-type potential in the following), and U_1 is the energy associated with the laser field. We shall use a linearly polarized laser field model, with polarization along the fixed z axis ($\theta=0$) of our spherical coordinate system—i.e.,

$$U_1=a_z r\cos\theta\cos\Psi(t). \tag{2}$$

Here, a_z is constant, while $\Psi(t)=\omega_0 t-\frac{1}{2}\alpha t^2$ is the phase of the driving field, where, for simplicity, we assume linear variation of the driving frequency with time, $\omega(t)=d\Psi/dt=\omega_0-\alpha t$, ω_0 and α being some resonant frequency and a chirp rate, respectively. It should be mentioned that at larger excitation amplitudes, particularly near the dissociation limit, the more complicated dependence of U_1 on r should be taken

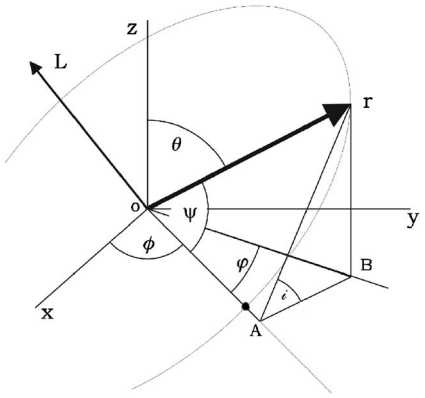

FIG. 1. Geometry of the classical 3D motion of the reduced mass μ. The z axis represents the direction of polarization of the laser field, **L** is the total angular momentum, i, ϕ, and ψ are the conventional Euler angles (OA is the line of nodes), while r, φ, and θ are spherical coordinates of the mass. The unperturbed motion of the mass is in the plane perpendicular to **L**

into account [10], but we shall neglect this effect in the present study for simplicity. The theory of autoresonance in the case of a more general elliptical polarization can be developed similarly (the case of circular polarization is discussed at the end of Sec. VI). In addition to spherical coordinates r, θ, and φ in Fig. 1, we also show the conventional Euler angles i, ϕ, and ψ describing the motion of μ in three dimensions and OA is the line of nodes, while **L** is the vector of the total angular momentum of the molecule.

The dynamics of the unperturbed ($U_1=0$) problem governed by Eq. (1) is integrable and comprises a quasiperiodic motion in a plane. We shall approach the perturbed molecule problem by transforming to the canonical action-angle variables of the *unperturbed* Hamiltonian. These variables are known to comprise the most convenient set of canonical coordinates and momenta for analyzing resonantly perturbed dynamics of integrable systems of many degrees of freedom. We define these canonical variables in our case in the Appendix, following the classical formulation in [11]. Here, we present only a necessary minimum of the results of this appendix.

There exist three canonical actions and three conjugated angles fully describing dynamics of the reduced mass in 3D. The convenient choices of the action variables are the total unperturbed angular momentum $I_2=|\mathbf{L}|$, the projection I_1 of **L** on the laser polarization axis (z axis in Fig. 1), and action I_3 associated with the radial vibrations. It is shown in the Appendix that the unperturbed Hamiltonian is a function of I_2 and I_3 only, $H_0=H_0(I_2,I_3)$. It is also shown in the Appendix that the conjugate angle Θ_1 coincides with the Euler angle ϕ, Θ_2 is related to another Euler angle ψ via $\Theta_2=\psi+V$, while V and radius r are 2π periodic in Θ_3 and functions of I_2 and I_3—i.e., $r=r(I_2,I_3,\Theta_3)$ and $\Theta_2=\Theta_2(I_2,I_3,\Theta_3)$. Thus, one can rewrite the perturbed Hamiltonian (1) in the form

$$H=H_0(I_2,I_3)+H_1(I_1,I_2,I_3,\Theta_2,\Theta_3), \tag{3}$$

where $H_1=a_z r(I_2,I_3,\Theta_3)\cos\theta\cos\Psi(t)$, which upon using the trigonometric relation (see triangles ABr and Aor in Fig. 1 for the derivation)

$$\cos\theta=\sin i\sin\psi=\sqrt{1-I_1^2/I_2^2}\sin[\Theta_2-V(I_2,I_3,\Theta_3)], \tag{4}$$

reduces to

$$H_1=a_z r(I_2,I_3,\Theta_3)\sqrt{1-I_1^2/I_2^2}\cos[\Theta_2-V(I_2,I_3,\Theta_3)]\cos\Psi(t). \tag{5}$$

III. AUTORESONANT CONTROL OF MOLECULAR DEGREES OF FREEDOM

At this stage we consider the dynamics of the molecule perturbed by chirped laser field in more detail. The dynamics is governed by Hamiltonian (3), which, at this point, is exact. Note that Θ_1 in this problem is a cyclic variable and, therefore I_1 remains constant of motion defined by initial conditions. Consequently, the problem reduces to perturbed dynamics of the remaining two pairs of canonical variables I_2,Θ_2 and I_3,Θ_3. Note that in the unperturbed case, the frequencies $\Omega_{2,3}=d\Theta_{2,3}/dt=\partial H_0/\partial I_{2,3}$ are the rotational and vibrational frequencies, respectively. At the same time $\Omega_1=d\Theta_1/dt=\partial H_0/\partial I_1=0$, but, in the driven case $d\Theta_1/dt\neq 0$ and describes a slow precession of the orbital plane around the polarization axis of the driving field. Approximations are necessary for making progress in this problem. We shall be interested in resonant interactions and, therefore, analyze the reduced two degrees of freedom problem within the single-resonance approximation [12]. To this end, we observe that H_1 can be expressed as

$$H_1=\mathrm{Re}\{a[e^{i(\Theta_2+\Psi)}+e^{i(\Theta_2-\Psi)}]\}, \tag{6}$$

where complex coefficient

$$a=a_z r(I_2,I_3,\Theta_3)\sqrt{1-I_1^2/I_2^2}\exp[-iV(I_2,I_3,\Theta_3)] \tag{7}$$

is 2π periodic in Θ_3. The single-resonance approximation is based on expanding a in a Fourier series, $a=\Sigma a_m\exp(im\Theta_3)$, and leaving only a single term in this expansion combined with one of the exponentials $e^{i(\Theta_2\pm\Psi)}$ in Eq. (6), in order to describe a particular resonance in the problem. For example, in the case of $\omega\approx\Omega_2$ (purely rotational resonance), we neglect exponential $e^{i(\Theta_2-\Psi)}$ in H_1 and leave the term a_0 only in the Fourier expansion of a. This yields a single-resonance Hamiltonian of form

$$H_{1r}=\mathrm{Re}\{a_0(I_2,I_3)\exp[i(\Theta_2-\Psi)]\}=b\cos(\Theta_2-\Psi+\eta),$$

where b and η are the absolute value and phase of a_0, both functions of I_2,I_3. More generally, for studying the resonant dynamics associated with resonances $\Omega_2+m\Omega_3\pm\omega\approx 0$ in our system, we use the single-resonance Hamiltonian

$$H_{1r}=b\cos(\Theta_2+m\Theta_3\pm\Psi+\eta),$$

with a particular choice of m and sign at Ψ. The idea behind the single-resonance approximation is the expected significant effect of the perturbing term having resonant (slowly varying) phase argument $\Theta_2+m\Theta_3\pm\Psi$ on the long-time evolution of the system, as compared to nonresonant perturbing terms with rapidly varying phases, yielding a small averaged contribution in the dynamics. Two examples of resonant dynamics are considered next.

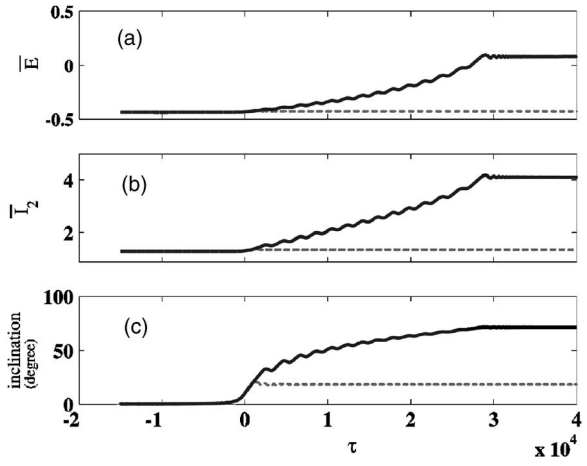

FIG. 2. Autoresonant evolution. (a) Normalized energy $\bar{E}$, (b) angular momentum $\bar{I}_2$, and (c) inclination i versus normalized time τ. The dashed and solid lines correspond to driving amplitudes just below and above the threshold for synchronization, respectively.

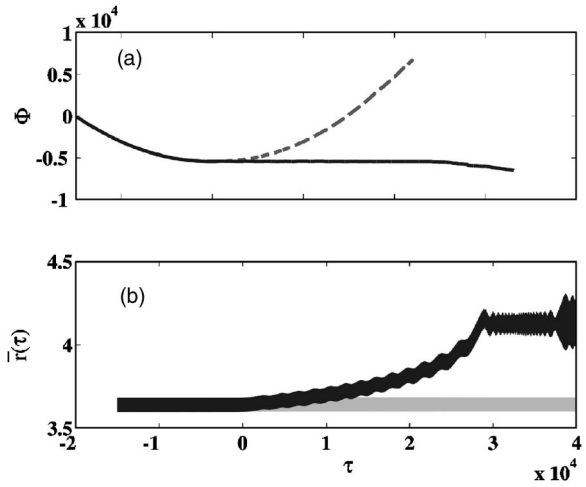

FIG. 3. The phase locking and radial evolution. (a) Phase mismatch Φ versus normalized time τ above (solid line) and below (dashed line) the threshold. (b) Normalized radius $\bar{r}$ versus time [above threshold (black), below threshold (gray)].

A. Rotational autoresonance

Here we focus on $\omega \approx \Omega_2$ (purely rotational resonance) and consider dynamics governed by

$$H_r = H_0(I_2, I_3) + b(I_2, I_3)\cos\Phi, \tag{8}$$

where phase mismatch $\Phi = \Theta_2 - \Psi(t) + \eta(I_2, I_3)$. We observe that Θ_3 is a cyclic variable; i.e., I_3 (vibrational action) is a constant of motion. Therefore, the problem reduces to that of one degree of freedom for the canonical pair I_2, Θ_2. Hamiltonian H_r yields the evolution equations

$$dI_2/dt = b\sin\Phi, \tag{9}$$

$$d\Phi/dt = \Omega_2 - \omega(t) - d\eta/dt + (db/dI_2)\cos\Phi. \tag{10}$$

This is the desired set describing autoresonance in our problem. An analysis of a similar system can be found elsewhere [13,14], and here we shall present only the main results of this theory. Suppose one starts in exact resonance $\omega(t_0) = \Omega_2$ at some initial time t_0. Then, if the driving frequency chirp rate $d\omega/dt$ is small enough, the system will stay in an approximate resonance $\omega(t) \approx \Omega_2(I_2)$ continuously, despite variation of the driving frequency, by automatically adjusting its action I_2 in the process of evolution. This important result of autoresonance theory means efficient control of I_2 by simply chirping the laser frequency. A more detailed analysis shows that in autoresonance, the action I_2 can be written as $I_2 = \bar{I}_2 + \delta I_2$, where $\bar{I}_2(t)$ is a smooth monotonically changing component satisfying the exact resonance relation $\omega(t) = \Omega_2(\bar{I}_2)$, while δI_2 is a small, $O(|b|^{1/2})$, component oscillating at frequency $\nu \sim \sqrt{|b(d\Omega_2/d\bar{I}_2)|}$. Similarly, the phase mismatch is given by $\Phi = \bar{\Phi} + \delta\Phi$, where $\bar{\Phi} \sim \nu^{-2} d\omega/dt$ (assumed to be small) is a smooth slowly evolving component, while $\delta\Phi$ oscillates with frequency ν. Thus, in autoresonance, Φ remains bounded throughout the evolution process, meaning continuing phase locking in the system. Finally, as the variation of the driving frequency continues, the rotational action I_2 may approach dissociation limit, where stochastic dissociation can take place at later times (see Figs. 2 and 3). A similar stochastic ionization phenomenon in Rydberg atoms in the developed autoresonant excitation stage was discussed in Refs. [4,9].

B. Rotational-vibrational autoresonance

Here we consider another possible resonance in our system—i.e., $\omega \approx \Omega_2 + \Omega_3$. The single-resonance Hamiltonian in this case has the same form as Eq. (8), but, now, $\Phi = \Theta_2 + \Theta_3 - \Psi(t) + \eta(I_2, I_3)$, while b and η are associated with a different Fourier coefficient. The evolution of the driven system is then given by

$$dI_2/dt = b\sin\Phi, \quad dI_3/dt = b\sin\Phi, \tag{11}$$

$$d\Phi/dt = \Omega_2 + \Omega_3 - \omega(t) - \frac{d\eta}{dt} + \left(\frac{db}{dI_2} + \frac{db}{dI_3}\right)\cos\Phi. \tag{12}$$

The first two equations above yield a conservation law $I = I_3 - I_2 = \text{const}$, allowing us to express $I_2 = I_3 - I$, reducing the problem to a one-degree-of-freedom system of type of Eqs. (9) and (10) discussed above. Then, again, if one starts in the exact resonance $\omega(0) = \Omega_2 + \Omega_3$ and the frequency chirp is slow enough, the system will remain in autoresonance $\omega(t) \approx \Omega_2 + \Omega_3$ continuously. In other words its vibrational and rotational action variables $I_{2,3}$ will automatically adjust themselves, as the driving frequency varies in time. This means control of VR degrees of freedom by the chirped laser field. These conclusions are independent of the actual time dependence of the chirp rate provided it is small enough. Also, in autoresonance, the system can be returned to its initial state by simply reversing the direction of the variation of the laser frequency. Finally, in the developed VR autoresonance stage, the molecule may again adiabatically approach the stochastic dissociation limit.

Both examples above assumed initial phase locking (exact resonance) in the system. In practical terms this would require accurate knowledge of initial conditions and fine-tuning of the laser field. Remarkably, in certain cases, *passage through resonances* may lead to efficient capture of the system into resonance and subsequent autoresonant control of the molecule by a chirped laser field in the process of evolution. This resonant capture phenomenon was studied previously in a variety of dynamical applications [14], most recently in controlling the eccentricity and inclination of Rydberg atoms [9]. We discuss similar problems in the next section in association with the 3D autoresonant control of VR degrees of freedom of diatomic molecules.

IV. PASSAGE THROUGH RESONANCES

Here we consider the process of passage through and capture into nonlinear VR resonances at *small* initial excitations. We want to establish a condition for the efficient capture into resonance and to investigate how the interaction between rotational and vibrational degrees of freedom may affect this condition. To this end, we seek an expression for the *weakly nonlinear* Hamiltonian in the problem in terms of action-angle variables. We proceed by specifying the Morse potential $U_0=D\{1-\exp[-(r-r_0)/A]\}^2$, where r_0 is the equilibrium distance between the atoms, while A and D characterize the width and the depth of the potential well, respectively. We shall neglect rotational effects first. Then, for small vibrational excitation energies E—i.e., for $\varepsilon_v \equiv E/D \ll 1$—the energy dependence on the radial action I_3 and the relation between r and the radial action-angle variables are well known [15]:

$$E(I_3) = \varepsilon_v D = \omega_3 I_3 \left(1 - \frac{\omega_3 I_3}{4D}\right), \tag{13}$$

$$r(I_3,\Theta_3) = r_0 + A \ln\left(\frac{1+\sqrt{\varepsilon_v}\cos\Theta_3}{1-\varepsilon_v}\right), \tag{14}$$

where $\omega_3=\sqrt{2D/\mu A^2}$ is the linear vibrational frequency. Expanding Eq. (14) in a power series with respect to small parameter $\sqrt{\varepsilon_v}$ we obtain

$$\approx r_0\left[1+\beta\left(\sqrt{\varepsilon_v}\cos\Theta_3 - \frac{1}{4}\varepsilon_v\cos 2\Theta_3 + \frac{3}{4}\varepsilon_v\right)\right], \tag{15}$$

where $\beta=A/r_0$. Next, we include small rotational effects for calculating first-order amplitudes $v_{\pm 1}(I_2,I_3)$ in a Fourier series in expression (A9) for Θ_2. Since v_1 is independent of I_1, we can evaluate it in the case of zero inclination. In this case,

$$\frac{d\psi}{dt} = \frac{d\varphi}{dt} = \frac{I_2}{\mu r^2}. \tag{16}$$

Inserting the approximation for r from Eq. (15) into Eq. (16), expanding it to second order in $\sqrt{\varepsilon_v}$, and keeping the zero and first-harmonic terms only, we find the angular frequency

$$\frac{d\psi}{dt} \approx \frac{I_2}{\mu r_0^2}\left[1 - \frac{3\beta(1-\beta)\varepsilon_v}{2} - 2\beta\sqrt{\varepsilon_v}\cos\Theta_3\right]. \tag{17}$$

On the other hand, one can differentiate Eq. (A9) and obtain an alternative expression for $d\psi/dt$:

$$\frac{d\psi}{dt} \approx \frac{d\Theta_2}{dt} - i\frac{d\Theta_3}{dt}[v_1 e^{i\Theta_3} - v_{-1}e^{-i\Theta_3}]. \tag{18}$$

Comparing the two expressions (17) and (18) and recalling that $d\Theta_{2,3}/dt=\Omega_{2,3}$, we obtain

$$v_1 = v_{-1}^* = -i\frac{I_2}{\mu r_0^2 \Omega_3}\beta\sqrt{\varepsilon_v(I_3)}, \tag{19}$$

and find the lowest-order correction in Ω_2 due to vibrations:

$$\Omega_2 = \frac{\partial H_0}{\partial I_2} \approx \frac{I_2}{\mu r_0^2}\left[1 - \frac{3}{2}\beta(1-\beta)\varepsilon_v(I_3)\right]. \tag{20}$$

Finally, we combine Eqs. (13) and (20), yielding the lowest-order, weakly nonlinear unperturbed Hamiltonian for studying small excitations:

$$H_0(I_2,I_3) = \varepsilon_v(I_3)D + \frac{I_2^2}{2\mu r_0^2}\left[1 - \frac{3}{2}\beta(1-\beta)\varepsilon_v(I_3)\right]. \tag{21}$$

The next, $O(I_2^4)$, correction in the Hamiltonian is due to the centrifugal expansion of the molecule. By calculating the energy at the minimum of the effective potential $U_{eff}=U_0+I_2^2/2\mu r^2$ one finds that this correction is $-(\beta^2/D)(I_2^2/2\mu r^2)^2$, so, finally,

$$H_0 = D\left\{\varepsilon_v + \varepsilon_r\left[1 - \frac{3}{2}\beta(1-\beta)\varepsilon_v - \beta^2\varepsilon_r\right]\right\}, \tag{22}$$

where $\varepsilon_r=I_2^2/2D\mu r_0^2$. We consider several scenarios of capture into resonance next.

A. Capture into rotational autoresonance

Let the molecule be in a purely rotational state initially ($I_3=0$) and drive it by linearly polarized laser field, such that the chirped driving frequency $\omega=\omega_0-\alpha t$ passes rotational resonance $\omega_0=\Omega_2$ at $t=0$. The perturbing component H_1 in the Hamiltonian in this case is given by Eq. (6), where, to lowest order, $a=a_z r_0\sqrt{1-I_1^2/I_2^2}$. This yields the following single-resonance Hamiltonian for studying passage through $\omega\approx\Omega_2$ resonance:

$$H_r = H_0(I_2,I_3) + \frac{1}{2}a_z r_0\sqrt{1-\frac{I_1^2}{I_2^2}}\cos\Phi, \tag{23}$$

where the phase mismatch is $\Phi=\Theta_2-\Psi(t)$. This Hamiltonian gives the following evolution equations:

$$dI_1/dt = dI_3/dt = 0 \Rightarrow I_1 = \text{const}, \quad I_3 = 0, \tag{24}$$

$$\frac{dI_2}{dt} = \frac{a_z r_0}{2}\sqrt{1 - I_1^2/I_2^2}\,\sin\Phi, \tag{25}$$

$$\frac{d\Phi}{dt} = \Omega_2(I_2) - \omega(t) + \frac{a_z r_0}{2\sqrt{1 - I_1^2/I_2^2}}\frac{I_1^2}{I_2^3}\cos\Phi, \tag{26}$$

where, according to Eq. (22),

$$\Omega_2(I_2) = \partial H_0/\partial I_2 = D(\partial\varepsilon_r/\partial I_2)(1 - 2\beta\varepsilon_r). \tag{27}$$

Equations (25) and (26) comprise small-amplitude limits of the more general equations (9) and (10), discussed above. Now, consider the case of small inclinations—i.e., $I_2 \approx I_1$. Then, by writing $I_2 = I_1 + \delta$, replacing $\sqrt{1 - I_1^2/I_2^2} \approx i$ in Eqs. (25) and (26), and defining a new dependent variable $J = i^2 \approx 2\delta/I_1$, we arrive at the following set of equations describing passage through resonance in the problem:

$$\frac{\partial J}{\partial\tau} = \frac{\bar{a}_z}{\beta\bar{I}_1}\sqrt{J}\,\sin\Phi, \tag{28}$$

$$\frac{\partial\Phi}{\partial\tau} = \gamma J - \bar{\alpha}\tau + \frac{\bar{a}_z}{2\beta\bar{I}_1}\frac{1}{\sqrt{J}}\cos\Phi. \tag{29}$$

Here we assumed passage of the driving frequency $\omega(t) = \omega_2 - \alpha t$ through linear resonance $\Omega_2(I_2) = \omega_2$ at $t = 0$ and transformed to the following *dimensionless* variables and parameters: time $\tau = t\omega_3$, driving amplitude $\bar{a}_z = (a_z A/2D)$, angular momentum $\bar{I}_1 = I_1/I_0 = I_1/(2D/\omega_3)$, chirp rate $\bar{\alpha} = \alpha/\omega_3^2$, and nonlinear frequency shift coefficient

$$\gamma = \left(\frac{\delta}{\omega_3}\frac{\partial\Omega_2}{\partial\delta}\right)_{\delta=0} = 0.5\beta^2\bar{I}_1(1 - 6\beta^4\bar{I}_1^2).$$

Remarkably, this set of equations is generic for a large variety of autoresonant problems involving passage through resonance [14]. It predicts *efficient capture* into resonance and subsequent phase locking in the system, provided the driving parameter $\bar{a}_z/2\beta\bar{I}_1$ exceeds the threshold, $\bar{a}_z^{th}/2\beta\bar{I}_1 = 0.41\bar{\alpha}^{3/4}\gamma^{-1/2}$ [14]. Solving for the dimensionless driving amplitude we get

$$\bar{a}_z^{th} = 0.82\sqrt{2\bar{I}_1}\bar{\alpha}^{3/4}(1 - 6\beta^4\bar{I}_1^2)^{-1/2}. \tag{30}$$

The synchronization for $a_z > a_z^{th}$ yields the continuing growth of both the inclination and the total angular momentum (since $I_1 = L_z$ is a constant of motion), going beyond the small-inclination stage described by Eqs. (28) and (29), while the vibrational action I_3 remains small during the whole excitation process. This fully nonlinear autoresonant evolution was already discussed above. Thus, the passage and capture into resonance yields the possibility of adiabatic control of molecular rotation without exciting the vibrational degree of freedom. Figures 2 and 3 illustrate this possibility in numerical simulations. Figure 2 shows normalized energy $\bar{E} = (E - D)/2D$, angular momentum $\bar{L} = L(2D/\omega_3)$, and inclination i versus normalized time $\tau = t\omega_3$ in two cases, slightly above and below the calculated threshold, $\bar{a}_z^{th} \approx 1.44 \times 10^{-4}$. The solid lines in the figure correspond to $\bar{a}_z = 1.5 \times 10^{-4}$ (above the threshold), while for the dashed lines $\bar{a}_z = 1.40 \times 10^{-4}$ is below the threshold. The parameters in the simulations were $\bar{r}_0 = r_0/A = 1/\beta = 3.6$, $\bar{I}_1 = 1.3$, and $\bar{\alpha} = -5 \times 10^{-6}$. We see in the figure that above the threshold, the energy, angular momentum, and inclination of the molecule increase after passage through resonance, as the driving frequency increase until the molecule dissociates. Figure 3 illustrates capture into resonance in the aforementioned example followed by continuing phase locking in the system, showing that the phase mismatch remains bounded in the autoresonant stage of interaction until dissociation. One can also see in the figure that the normalized radius $\bar{r}$ increases during the interaction, but lacks vibrational oscillations; i.e., the purely rotational degree of freedom is excited throughout the excitation process in this case.

B. Capture into VR autoresonance

Again, we proceed with the molecule in a purely rotational state ($I_3 = 0$) and drive it by linearly polarized laser field, but in contrast to the previous example, assume that the chirped laser frequency $\omega = \omega_0 - \alpha t$ passes through one of the combination resonances $\omega_0 = \Omega_2 \pm \Omega_3$ at $t = 0$. The perturbing component H_1 in the Hamiltonian is still given by Eqs. (6) and (7), but now, in calculating the relevant Fourier component of $a = a_z r\sqrt{1 - I_1^2/I_2^2}\exp[-iV]$, to lowest order, $r \approx r_0 + \beta\sqrt{\varepsilon_v}\cos\Theta_3$, $\varepsilon_v \approx \omega_3 I_3/D$, and $V \approx v_1\exp(i\Theta_3) + \text{c.c.}$, where $v_1 \approx -i\beta(\omega_2/\omega_3)\sqrt{\varepsilon_v}$—i.e.,

$$a_\pm \approx \frac{1}{2}a_z r_0\beta\sqrt{\omega_3 I_3/D}\sqrt{1 - \frac{I_1^2}{I_2^2}}\left(\frac{1}{2} \mp \frac{\omega_2}{\omega_3}\right)\exp(\pm i\Theta_3).$$

This result yields the following single-resonance Hamiltonians for studying passage through $\omega \approx \Omega_2 \pm \Omega_3$ resonances:

$$H_r = H_0(I_2, I_3) + 2\epsilon^\pm\sqrt{1 - I_1^2/I_2^2}\sqrt{I_3}\cos\Phi_\pm, \tag{31}$$

where $\epsilon^\pm = \frac{1}{4}a_z r_0\beta\sqrt{\omega_3/D}\left(\frac{1}{2} \mp \omega_2/\omega_3\right)$ and $\Phi_\pm = \Theta_2 \pm \Theta_3 - \Psi(t)$. It should be mentioned that the case of small rotations ($\Omega_2 \approx 0$) requires special attention, since the two resonant frequencies $|\Omega_2 \pm \Omega_3|$ are nearly the same in this case and, therefore, the single-resonance approximation as used above may not be valid in this case. We shall discuss this important limit at the end of this section.

Now, we analyze the dynamics governed by Eq. (31). We observe that I_1 is a constant of motion and focus on the case $I_1 = 0$ (polarization of the laser field is in the plane of motion) for simplicity. We can write down dimensionless evolution equations for this case,

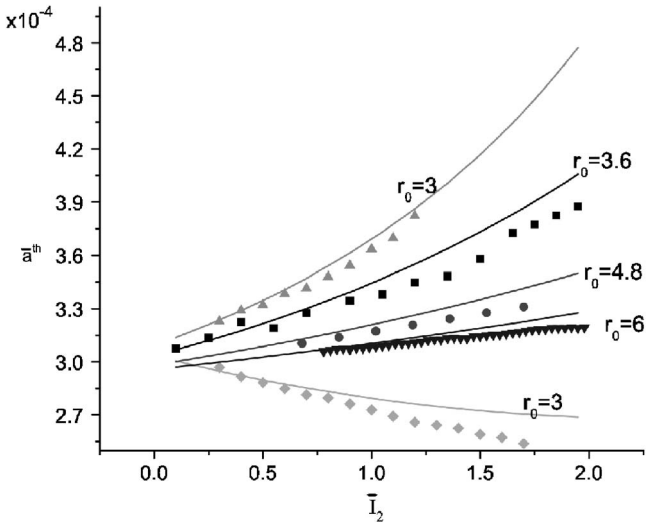

FIG. 4. The normalized threshold amplitude $\bar{a}_+^{th}$ as a function of initial rotational action $\bar{I}_2(0)$ for different values of initial normalized radius $\bar{r}_0$ in the case of $\omega(t) \simeq \Omega_2 - \Omega_3$ resonance. Gray triangles, black squares, black circles, and black triangles show the simulation results, while solid lines represent theoretical predictions. Also shown is the $\bar{a}_-^{th}$ threshold in the case of $\omega(t) \simeq \Omega_2 + \Omega_3$ resonance at $r_0 = 3.6$ in simulations (gray diamonds) and theory (solid line).

$$\frac{d\bar{I}_2}{d\tau} = 2\left[\frac{\bar{a}_\pm}{2\sqrt{2}}\left(\frac{1}{2} \mp \bar{\omega}_2\right)\right]\sqrt{\bar{I}_3}\sin\Phi_\pm, \tag{32}$$

$$\frac{d\bar{I}_3}{d\tau} = \pm 2\left[\frac{\bar{a}_\pm}{2\sqrt{2}}\left(\frac{1}{2} \mp \bar{\omega}_2\right)\right]\sqrt{\bar{I}_3}\sin\Phi_\pm, \tag{33}$$

$$\frac{d\Phi_\pm}{d\tau} = \bar{\Omega}_2 \pm \bar{\Omega}_3 - \bar{\omega}(t) \pm \left[\frac{\bar{a}_\pm}{2\sqrt{2}}\left(\frac{1}{2} \mp \bar{\omega}_2\right)\right]\frac{1}{\sqrt{\bar{I}_3}}\cos\Phi_\pm, \tag{34}$$

where $\bar{I}_{2,3} = I_{2,3}/I_0$ are dimensionless actions ($I_0 = 2D/\omega_3$), $\bar{a}_\pm = a_\pm A/2D$ is the dimensionless driving amplitude, and, again, $\tau = \omega_3 t$ is the dimensionless time. Taking either $\bar{a}_+ = 0$ or $\bar{a}_- = 0$, the first two equations in this set yield the conservation law $\bar{J}_\pm = \bar{I}_2 \pm \bar{I}_2 = \text{const}$. This allows us in both cases to express $\bar{I}_2$ in Eq. (34) via $\bar{I}_3$ and reduce Eqs. (33) and (34) to the standard form [compare to Eqs. (28) and (29)]

$$\frac{d\bar{I}_3}{d\tau} = \pm 2\left[\frac{\bar{a}_\pm}{2\sqrt{2}}\left(\frac{1}{2} \mp \bar{\omega}_2\right)\right]\sqrt{\bar{I}_3}\sin\Phi_\pm,$$

$$\frac{d\Phi_\pm}{d\tau} = \gamma_\pm \bar{I}_3 - \bar{\alpha}\tau \pm \left[\frac{\bar{a}_\pm}{2\sqrt{2}}\left(\frac{1}{2} \mp \bar{\omega}_2\right)\right]\frac{1}{\sqrt{\bar{I}_3}}\cos\Phi_\pm,$$

where the coefficient $\gamma_\pm$ characterizing the lowest-order nonlinear frequency shift is

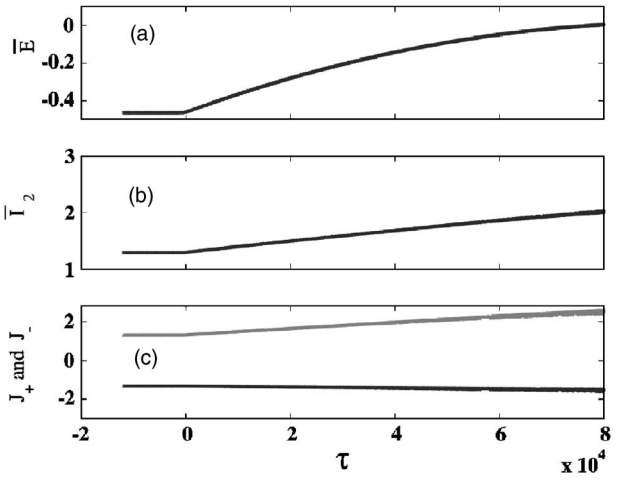

FIG. 5. The normalized energy $\bar{E}$, angular momentum $\bar{I}_2$, $\bar{J}_+$ [(c), upper trace] and $\bar{J}_-$ [(c), lower trace] versus normalized time τ in the case of $\omega(t) \simeq \Omega_2 + \Omega_3$ autoresonance.

$$\gamma_\pm = 1 - \beta^2 \pm 6\beta(1-\beta)\bar{\omega}_2 - \frac{3}{2}\left(\frac{1-\beta}{\beta}\right)\bar{\omega}_2^2 + 24\beta^2\bar{\omega}_2^2. \tag{35}$$

This system again yields the autoresonant threshold phenomenon and, similarly to our previous example, predicts efficient capture into resonance followed by autoresonant evolution with vibrational energy growing in time, provided the driving amplitude $\bar{a}_\pm$ exceeds a threshold—i.e.,

$$\bar{a}_\pm > \bar{a}_\pm^{th} = 1.16\bar{\alpha}^{3/4}\gamma_\pm^{-1/2}\left(\frac{1}{2} \mp \bar{\omega}_2\right)^{-1}. \tag{36}$$

We compare this result for the threshold with simulations in Fig. 4, showing $\bar{a}_+^{th}$ (and in one case, gray diamonds, $\bar{a}_-^{th}$) versus the initial angular momentum $\bar{I}_2(0)$, as found in theory and simulations for different values of $\bar{r}_0$. A good agreement between the theory and simulations can be seen in the figure. As the vibrational energy increases in autoresonance and molecular rotation adjusts itself according to $I_2 = J_\pm \pm I_3$, one may reach values of $I_{2,3}$ beyond the weakly nonlinear theory. This large excitation case was already discussed above. Finally, inclusion of finite initial inclination ($I_1 \neq 0$) does not change the theory significantly, since I_1 as well as $J_\pm = I_2 \pm I_3$ remain constants of motion. Nevertheless, since I_2 varies with the vibrational energy, the inclination $i = \sin^{-1}\sqrt{1 - I_1^2/I_2^2}$ of the orbital plane in the $I_1 \neq 0$ case experiences slow autoresonant evolution, while the orbital plane itself performs slow precession around the polarization vector of the laser field.

Next, we illustrate the whole VR autoresonance process in simulations using parameters $\bar{r}_0 = 3.6$, $\bar{I}_2(0) = 1.3 \Rightarrow \bar{\omega}_2 = 0.1$, $\bar{\alpha} = 1 \times 10^{-5}$, $\bar{a}_+ = 5 \times 10^{-4}$, and $\bar{a}_- = 4 \times 10^{-4}$. Figure 5 shows the results of the simulation in the $\bar{\omega}(\tau) \simeq \bar{\Omega}_2 + \bar{\Omega}_3$ case. We see that the normalized energy, angular momentum, and $\bar{J}_+ = \bar{I}_2 + \bar{I}_3$ are increasing in time, while $\bar{J}_-$ remains almost constant. Figure 6 shows the results of the numerical simulation

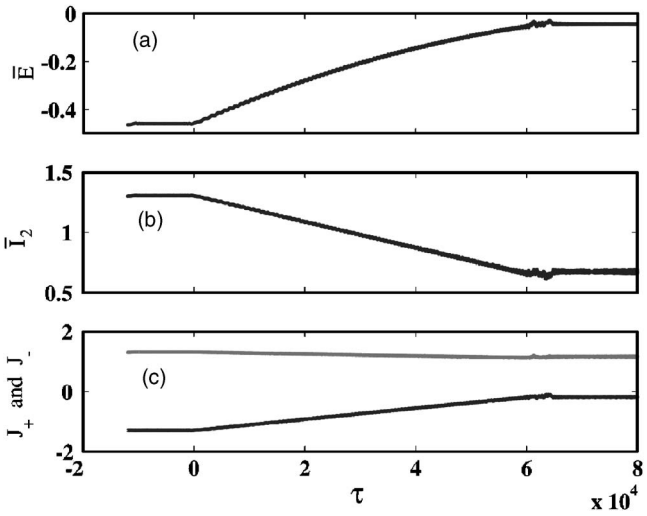

FIG. 6. The normalized energy $\bar{E}$, angular momentum $\bar{I}_2$, $\bar{J}_+$ [(c), upper trace] and $\bar{J}_-$ [(c), lower trace] versus normalized time τ in the case of $\omega(t) \simeq \Omega_2 - \Omega_3$ autoresonance.

of the VR autoresonance in the $\bar{\omega}(\tau) \simeq \bar{\Omega}_2 - \bar{\Omega}_3$ case. We see that the normalized energy and $\bar{J}_- = \bar{I}_2 - \bar{I}_3$ in this case are increasing in time, while, as expected, $\bar{J}_+$ remains almost constant. As a consequence, in contrast to the $\bar{\omega}(\tau) \simeq \bar{\Omega}_2 + \bar{\Omega}_3$ case, while the total energy is increasing, the angular momentum decreases during this process. We can view this effect as "heating" of the vibrational degree of freedom while "cooling" the rotational degree of freedom, possibly useful in applications.

As the last illustration, we estimate autoresonance parameters and threshold in the case of a realistic HF molecule with the following parameters: $r_0 = 0.917$ Å, $A = 0.451$ Å $\Rightarrow \beta = 0.491$, $\bar{\nu}_3 = 4138\ \mathrm{cm}^{-1}$, $\bar{\nu}_2 = 20.56\ \mathrm{cm}^{-1}$, $D = 6.125$ eV, and $q \approx 0.35e$ (q is the effective charge, e the electron charge) [7,16]. Taking a radiation source with pulse duration of 1 psec and bandwidth of 270 cm^{-1}, we find $\bar{\alpha} = 8.37 \times 10^{-5}$. Assuming that at room temperature one can neglect $\bar{\omega}_2$ (for detailed discussion of the validity of this approximation see below), Eqs. (35) and (36) yields

$$\bar{a}^{th} = 2.32 \frac{\bar{\alpha}^{3/4}}{\sqrt{1-\beta^2}} = 2.3 \times 10^{-3}. \tag{37}$$

The corresponding electric field is $E_{th} = \bar{a}^{th}(2D/qA)$, yielding threshold intensity

$$I^{th} = \frac{c}{8\pi} E_{th}^2 = 4 \times 10^{11}\ \mathrm{W/cm}^2. \tag{38}$$

We can also calculate the purely rotational threshold given in Eq. (30) for the HF molecule. Setting $I_1^2/(2\mu r_0^2) = \beta^2 \bar{I}_1^2 D \approx k_B T$ we have $\bar{I}_1 = 0.13$ (k_B is the Boltzmann constant, and T is the room temperature). Plugging it into Eq. (30) yields $\bar{a}_{rot}^{th} = 3.6 \times 10^{-4}$ and threshold intensity $I^{th} = 1.0 \times 10^{10}\ \mathrm{W/cm}^2$.

Finally, we discuss the $\bar{\omega}_2 = 0$ limit in more detail. As mentioned earlier the resonant frequencies $|\Omega_2 \pm \Omega_3|$ coincide in this limit and our single-resonance approximation, formally, is invalid. Nevertheless, we observe that the single-resonance approximation used in Eq. (31) is equivalent to separating the linearly polarized laser field into two opposite circularly polarized laser field components and leaving only one of them in the Hamiltonian. Therefore, if one replaces the linearly polarized laser field in by a circularly polarized field of proper direction of rotation, there is no need in the single-resonance approximation in the theory. Furthermore, by using circularly polarized light, we reduce the threshold amplitude calculated in Eq. (36) by factor of 2—i.e., obtain the condition

$$\bar{a}_{\mathrm{circ}}^{th} = 0.58 \bar{\alpha}^{3/4} \gamma_{\pm}^{-1/2} \left(\frac{1}{2} \mp \bar{\omega}_2 \right)^{-1}. \tag{39}$$

This result allows taking zero-initial-rotation limit ($\bar{\omega}_2 = 0$), yielding

$$\bar{a}_{\mathrm{circ}}^{th} \to 1.16 \frac{\bar{\alpha}^{3/4}}{\sqrt{1-\beta^2}}.$$

If one insists on using linearly polarized radiation, one must consider the problem of the overlap of resonances. This introduces a condition on the smallness of $\bar{\omega}_2$ for using the single-resonance approximation. Indeed, for the validity of the single-resonance approximation, we require the difference between $\bar{\Omega}_+ = \bar{\Omega}_3 + \bar{\Omega}_2$ and $\bar{\Omega}_- = \bar{\Omega}_3 - \bar{\Omega}_2$ to be larger than the width of the resonance [17]

$$\Delta_{res} \approx 4 \sqrt{\frac{\bar{a}_z}{2\sqrt{2}} \frac{1}{1-\beta^2}},$$

i.e., demand that $\Delta_{res} < 2\bar{\omega}_2$. On the other hand, we have condition (36) for efficient autoresonance. Combining these two conditions we find that $\bar{\omega}_2$ must satisfy the following inequality for efficient VR excitation by linearly polarized laser light:

$$\bar{\omega}_2^2 > 1.64 \bar{\alpha}^{3/4} (1-\beta^2)^{-3/2}. \tag{40}$$

If $\bar{\omega}_2$ is below this value, we expect the resonance overlap to destroy the autoresonant phase locking in the system in the 3D case with a linearly polarized laser field. It should be noted that similar conclusions were reached using quantum calculations [7].

For illustration, let us again consider the example of the HF molecule. Inserting the above-mentioned parameters into Eq. (40) we find $\bar{\omega}_2 = 0.047$. This rotation is equivalent to placing the molecule in the tenth rotational level for efficient capture into autoresonance. However, the use of a circularly polarized source allows us to avoid this preexcitation condition, reducing, at the same time, the threshold intensity given in Eq. (38) by a factor of 4.

V. CONCLUSIONS

In summary, we have shown that one can efficiently control the purely rotational state of the molecule by passage

through $\omega(t) \approx \Omega_2$ resonance. One can also efficiently manipulate a mixed RV state by adiabatic passage through $\omega(t) \approx \Omega_2 \pm \Omega_3$ resonances. Both scenarios are characterized by thresholds on the driving laser field amplitude for capture into resonance, which we calculated. The approach also allows different controls of ensembles of excited molecules. For example, one can align all molecules in the ensemble along a specific direction by autoresonant rotational excitation and control of inclination. We can also "cool down" the rotational degree of freedom of an ensemble, while "heating" the vibrational degree. A more complex scenario would be first aligning all the molecules by controlling inclination and then cooling down the rotations and exciting the vibrations. Since the capture into resonance and consequent continuing autoresonance (synchronization) in the system are insensitive to the initial phases of molecular vibrations and rotations, provided the initial vibrational energy is small enough, one expects capture and excitation of almost all molecules in the illuminated volume in these scenarios.

We have also investigated the role of the RV interaction on autoresonance and its effect on the efficiency of vibrational excitation. We have found that when using a linearly polarized chirped frequency light source, one needs a sufficient rotational preexcitation for efficient autoresonant vibrational excitation. Nevertheless, if instead of linearly polarized light one uses circular polarization, this condition is removed and the threshold on the driving field amplitude for capture into resonance is reduced by a factor of 2 (factor of 4 in intensity).

Finally, quantum mechanics requires all quantum numbers associated with quantized actions of the classical problem to be much greater than unity to justify a classical description. There may be other constraints dictated by quantum mechanics in the 3D case, which are presently unknown. The development of the quantum-mechanical theory of adiabatically phase-locked states described in this work and studying the transition from the quantum-mechanical ladder-climbing process to classical autoresonance in 3D comprises an important goal for future work.

ACKNOWLEDGMENT

This work was performed under the support of the Israel Science Foundation (Grant No. 187-02).

APPENDIX: UNPERTURBED ACTION-ANGLE VARIABLES

The unperturbed problem has three constants of motion, i.e., the total energy

$$E = \frac{1}{2\mu}\left(p_r^2 + \frac{p_\theta^2}{r^2} + \frac{p_\varphi^2}{r^2 \sin^2\theta}\right) + U_0,$$

the total angular momentum L, $L^2 = p_\theta^2 + p_\varphi^2/(r^2 \sin^2\theta)$, and the projection of the angular momentum on the z axis, $L_z = p_\varphi$. These three constants of motion enter the definitions of the following action variables:

$$I_\varphi = \frac{1}{2\pi}\oint L_z d\varphi = L_z, \tag{A1}$$

$$I_\theta = \frac{1}{2\pi}\oint \sqrt{L^2 - \frac{L_z^2}{\sin^2\theta}}\, d\theta = I_\theta(L, L_z), \tag{A2}$$

$$I_r = \frac{1}{2\pi}\oint \sqrt{2\mu(E - U_0) - \frac{L^2}{r^2}}\, dr = I_r(E, L). \tag{A3}$$

It can be shown [11] that Eq. (A2) yields

$$I_\theta = L - L_z = L - I_\varphi. \tag{A4}$$

Now, inverting Eq. (A3), we formally have

$$E = H_0(L, I_r) = H_0(I_\varphi + I_\theta, I_r). \tag{A5}$$

Equation (A5) shows that our unperturbed system is singly degenerate. In other words, if one introduces three canonical angle variables Θ_φ, Θ_θ, and Θ_r conjugate to I_φ, I_θ, and I_r, then the frequencies $d\Theta_\varphi/dt = \partial H_0/\partial I_\varphi$ and $d\Theta_\theta/dt = \partial H_0/\partial I_\theta$ of the unperturbed motion are the same. The convenient way of dealing with this degeneracy is transforming to a new set of action-angle variables—i.e., I_1, I_2, I_3 and $\Theta_1, \Theta_2, \Theta_3$—such that [11]

$$\Theta_1 = \Theta_\varphi - \Theta_\theta,$$

$$\Theta_2 = \Theta_\theta,$$

$$\Theta_3 = \Theta_r,$$

$$I_1 = I_\varphi,$$

$$I_2 = I_\theta + I_1 = L,$$

$$I_3 = I_r$$

The unperturbed Hamiltonian then becomes $H_0 = H_0(I_2, I_3)$ and, therefore, Θ_1 is a constant of motion. Explicit expressions for the new canonical angles and their physical interpretation can be obtained via the associated generating function [11]:

$$W = I_1\varphi + \int^\theta \sqrt{\left(I_2^2 - \frac{I_1^2}{\sin^2\theta}\right)}\, d\theta + \int^r \sqrt{2\mu(E - U_0) - \frac{I_2^2}{r^2}}\, dr. \tag{A6}$$

One can show that $\Theta_1 = \partial W/\partial I_1$ corresponds to the Euler angle ϕ between the x axis and the line of nodes associated with the plane of motion in the unperturbed problem, while $I_{1,2}$ define the inclination angle i (the third Euler angle) of the orbital plane, $\cos i = I_1/I_2$ (see Ref. [11] and illustration in Fig. 1).

The remaining two canonical angles are also derived from W—i.e., $\Theta_n = \partial W/\partial I_n$, $n = 2, 3$. We write an expression for Θ_3 first:

$$\Theta_3 = \sqrt{\frac{\mu}{2}} \int^r \frac{(\partial E/\partial I_3)dr}{\sqrt{(E-U_0) - I_2^2/r^2}}. \tag{A7}$$

Obviously, I_3, Θ_3 are action-angle variables describing oscillations of the radial variable r—i.e., the vibrational degree of freedom of the molecule. Inversion of Eq. (A7) shows that r is 2π periodic in Θ_3, as well as a function of I_2, I_3. Therefore, one can expand in a Fourier series

$$r(I_2, I_3, \Theta_3) = \bar{r} + \sum a_n(I_2, I_3)\exp(in\Theta_3), \tag{A8}$$

where $\bar{r}$ is the averaged distance between the two atoms. Next, we write $\Theta_2 = U + V$, where

$$U = I_2 \int^\theta \frac{d\theta}{\sqrt{I_2 - I_1/r^2}},$$

$$V = \int^r \left[\sqrt{\frac{\mu}{2}} \frac{\partial E}{\partial I_2} - \frac{I_2}{r^2} \right] \frac{dr}{\sqrt{2\mu(E-U_0) - I_2/r^2}}.$$

The function U in the last equation has a simple physical interpretation and reduces to the Euler angle ψ (see Fig. 1) between the radius vector and the line of nodes (see Ref. [11]), while V is a function of r and, therefore, 2π periodic in Θ_3. Thus, upon Fourier expansion,

$$\Theta_2 = \psi + \sum v_n(I_2, I_3)\exp(in\Theta_3). \tag{A9}$$

[1] J. C. Polanyi, Acc. Chem. Res. **5**, 161 (1972).
[2] D. J. Maas, D. I. Duncan, R. B. Vrijen, W. J. van der Zande, and L. D. Noordam, Chem. Phys. Lett. **290**, 75 (1998).
[3] S. Chelkowski, A. D. Bandrauk, and P. B. Corkum, Phys. Rev. Lett. **65**, 2355 (1990).
[4] B. Meerson and L. Friedland, Phys. Rev. A **41**, 5233 (1990).
[5] W. K. Liu, B. R. Wu, and J. M. Yuan, Phys. Rev. Lett. **75**, 1292 (1995).
[6] G. Marcus, L. Friedland, and A. Zigler, Phys. Rev. A **69**, 013407 (2004).
[7] S. Chelkowski and A. D. Bandrauk, J. Chem. Phys. **99**, 4279 (1993).
[8] J. H. Kim, W. K. Liu, F. R. W. McCourt, and J. M. Yuan, J. Chem. Phys. **112**, 1757 (2000).
[9] E. Grosfeld and L. Friedland, Phys. Rev. E **65**, 046230 (2002).
[10] J. N. Huffaker, M. Karimi, and L. B. Tran, J. Mol. Spectrosc. **124**, 393 (1987).
[11] H. Goldstein, *Classical Mechanics*, 2nd ed. (Addison-Wesley, Reading, MA, 1980).
[12] B. V. Chirikov, Phys. Rep. **52**, 264 (1979).
[13] L. Friedland, Phys. Rev. E **55**, 1929 (1997).
[14] J. Fajans and L. Friedland, Am. J. Phys. **69**, 1096 (2001).
[15] M. E. Goggin and P. W. Milonni, Phys. Rev. A **37**, 796 (1988).
[16] R. N. Sileo and T. A. Cool, J. Chem. Phys. **65**, 117 (1976).
[17] B. V. Chirikov and G. M. Zaslavksy, Usp. Fiz. Nauk **105**, 3 (1971).